

## Electron-phonon effects on the Raman spectrum in MgB<sub>2</sub>

E. Cappelluti

*Istituto dei Sistemi Complessi, CNR-INFN, v. dei Taurini 19, 00185 Roma, Italy  
and Dipart. di Fisica, Università di Roma "La Sapienza," P.le A. Moro, 2, 00185 Roma, Italy*

(Received 7 March 2006; published 24 April 2006)

The anomalous features of the Raman spectroscopy measurement in MgB<sub>2</sub> represent a still unresolved puzzle. In particular, highly debated are the origin of the huge  $E_{2g}$  phonon linewidth, the nature of the low energy ( $\omega < \omega_{E_{2g}}$ ) background and the evolution of the Raman spectra with Al doping. In this paper we compute the self-energy of the  $E_{2g}$  phonon mode in a fully self-consistent way, taking into account electron-phonon effects on the electronic properties. We show that all the anomalous features can be naturally understood in a framework where the whole electron-phonon spectrum  $\alpha^2 F(\omega)$  gives rise to significant damping processes for the electronic excitations and consequently for the  $E_{2g}$  phonon itself. The two-peak structure as function of the Al doping is ascribed to finite bandwidth effects arising as the Fermi level approaches the  $\sigma$  band edge.

DOI: 10.1103/PhysRevB.73.140505

PACS number(s): 74.70.Ad, 63.20.Kr, 74.25.Kc, 78.30.-j

There is nowadays a general consensus that the electron-phonon (el-ph) interaction is responsible for the superconductivity in MgB<sub>2</sub>.<sup>1-6</sup> Interesting peculiarities make, however, this compound quite unique and different from the conventional low- $T_c$  superconductors. Most notable are the two-bands/two-gaps phenomenology,<sup>4,6-11</sup> the fact that a large part of the electron-phonon coupling is concentrated in just one phonon mode  $E_{2g}$ ,<sup>1,3,5</sup> the possibility of spanning with Al doping a wide range of hole doping of the  $\sigma$  bands.<sup>12</sup> Although several features are now well understood within the context of the two-gaps scenario, the experimental overview of the Raman spectroscopy of this compound still represents a highly puzzling anomaly.<sup>13-19</sup> The main open questions on this point regard, in particular, the origin of the anomalously large linewidth of the  $E_{2g}$  phonon mode, the nature of the background Raman signal at low frequencies, and the evolution of the Raman spectra upon Al doping, which shows a transfer of spectral weight between different peaks more than a continuous hardening of the  $E_{2g}$  phonon mode.

In this Letter we show that all these unconventional features can be explained within the electron-phonon scenario by the coexistence of a strongly coupled ( $E_{2g}$ ) phonon mode at  $\mathbf{q}=0$  and of a wide background electron-phonon scattering with other phonon branches and different momenta. This gives rise to a Fano-like phenomenology, where the shape and linewidth of the  $E_{2g}$  mode is mainly related to the electron-phonon decay processes triggered by the other modes and by impurity scattering. Similar effects give rise to a low energy peak, equivalent to the Drude-like feature in the optical conductivity, which is responsible for the low energy signal. We show also that the transfer of spectral weight between different Raman structures as function of the Al amount can be a direct consequence of the vanishing of the Fermi energy.

The origin of the broad phonon linewidth in Raman spectroscopy has been widely discussed in literature.<sup>13,17,20-22</sup> The common feeling on this subject is that the linewidth of a phonon mode  $\gamma_{\mathbf{q}}$  reflects the strength of the electron-phonon

coupling  $\lambda_{\mathbf{q}}$  of this specific mode, in the spirit of the Allen's formula  $\gamma_{\mathbf{q}} = 2\pi N(0)\lambda_{\mathbf{q}}\omega_{\mathbf{q}}^2$ ,<sup>23</sup> where  $N(0)$  is the electron density of states (DOS) coupled with the phonon mode and  $\omega_{\mathbf{q}}$  is the phonon frequency. First-principle calculations, however, indicate that the electron-phonon coupling alone of the  $E_{2g}$  phonon mode is not sufficient to explain the large experimental Raman linewidth.<sup>22</sup> In addition, the direct employment of the Allen's formula is strongly questioned in the  $\mathbf{q}=0$  case, relevant for the Raman spectroscopy, where a more careful analysis shows that the damping of a  $\mathbf{q}=0$  phonon mode scattering with a *noninteracting* electronic system is strictly zero.<sup>22</sup>

In contrast to the above scenario, a Quantum Field Theory analysis specifically addressed to the  $\mathbf{q}=0$  case has been developed in Refs. 24 and 25. Although these studies were mainly aimed at investigating phonon anomalies in the superconducting state, this approach can be as well employed in the normal state. Along this line, for instance, Marsiglio *et al.* remarked<sup>25,33</sup> that the imaginary part of a  $\mathbf{q}=0$  phonon self-energy in the weak-coupling limit is simply

$$\Pi''(\mathbf{q}=0, \omega) \propto \omega_{\mathbf{q}} \lambda_{\mathbf{q}=0} \frac{4\omega \Gamma_{\text{imp}}}{\omega^2 + 4\Gamma_{\text{imp}}^2}, \quad (1)$$

where the impurity scattering rate  $\Gamma_{\text{imp}}$  was assumed to be the only damping source of the electronic propagator:  $G(\mathbf{k}, \omega) = 1/(\omega - \epsilon_{\mathbf{k}} + i\Gamma_{\text{imp}})$ .

Equation (1) explicitly shows that the damping processes of a  $\mathbf{q}=0$  phonon are triggered by corresponding damping processes of the electronic charge response that screens the phonon, whereas the el-ph coupling  $\lambda_{\mathbf{q}=0}$  of this particular mode rules the magnitude of these effects. This result holds true also when the main source of the the electronic excitation damping is the electron-phonon interaction itself. In this case it is also important to note that, in principle, all the phonon modes, and not only the specific  $\lambda_{\mathbf{q}=0}$  mode, contribute to the electronic damping. Indeed, as we are going to discuss, the imaginary part  $\Pi''(\omega)$  of the phonon self-energy is roughly related to the integral up to the energy  $\omega$  of the

imaginary part of the *electronic* self-energy,  $\gamma(\mathbf{q}=0, \omega) \propto \lambda_{\mathbf{q}=0} \int_0^\omega d\omega' \Gamma(\omega')$ . For optical phonons close to the top of the phonon spectrum, we have  $\int_0^\omega d\omega' \Gamma(\omega') \propto \lambda\omega$ ,  $\lambda$  being the *total* electron-phonon coupling constant, so that in intermediate-strongly coupled systems the phonon linewidth can be of the same order of the phonon frequency itself. In conventional low- $T_c$  superconductors, however, the total electron-phonon coupling  $\lambda \sim 1$  is spread over several phonon branches and  $\mathbf{q}$  modes,  $\lambda = \sum_{\mathbf{q}, \nu} \lambda_{\mathbf{q}, \nu}$ , so that the contribution from a single mode is quite small. Typical values of  $\lambda_{\mathbf{q}=0, \nu}$  for the  $A_g$  phonon modes in cuprates are, for instance,  $\lambda_{\mathbf{q}=0, \nu} \leq 0.034$ ,<sup>26</sup> resulting in experimental Raman linewidths of a few meV.<sup>27</sup> The opposite extreme case of only one strong coupled  $\mathbf{q}=0$  phonon mode  $\omega_0$  carrying the whole electron-phonon coupling would also predict an extremely small phonon linewidth since, although  $\lambda_{\mathbf{q}=0} \sim 1$ , the amount of electron-phonon coupling smaller than  $\omega_0$  is practically negligible, and  $\int_0^{\omega_0} d\omega \Gamma(\omega) \approx 0$ .

Along this scenario, MgB<sub>2</sub> presents very peculiar characteristics, since it presents at the same time two (degenerate) strong coupled  $\mathbf{q}=0$   $E_{2g}$  phonon modes *and* a relevant fraction of the total electron-phonon coupling strength spread over other different modes.<sup>1,3,5,6</sup> We employ a fully self-consistent many-body approach to investigate the normal state  $E_{2g}$  Raman spectrum of MgB<sub>2</sub>. In a more explicit way, we first solve iteratively the Marsiglio-Schossmann-Carbotte equations<sup>28</sup> with the Eliashberg spectral function  $\alpha_\sigma^2 F(\omega)$  obtained by first-principle calculations<sup>29</sup> (Fig. 1(a)) to evaluate the real-axis electronic self-energy  $\Sigma(\omega)$  of the  $\sigma$  bands. The Eliashberg function  $\alpha_\sigma^2 F(\omega) = \alpha_{\sigma\sigma}^2 F(\omega) + \alpha_{\sigma\pi}^2 F(\omega)$  describes the total electron-phonon scattering of the  $\sigma$  electrons with both the  $\sigma$  and  $\pi$  bands. Note that the  $\alpha^2 F(\omega)$  extracted from first-principle techniques represents the el-ph spectral function, where phonons are *already* renormalized. In order to better compare with the experiments, we include also explicitly the possible effects of impurity disorder. We schematize the  $\sigma$  bands as two degenerate bands with constant DOS, namely,  $\sum_{\mathbf{k}} G(\mathbf{k}, \omega) = N_\sigma(0) \int d\epsilon G(\epsilon, \omega)$ , where  $N_\sigma(0)$  represents the  $\sigma$ -band electron density of states per spin and per band,  $N_\sigma(0) \approx 0.075$  states/(eV cell).<sup>1,2</sup> The so-obtained electronic Green's function is then employed as input to calculate the full frequency dependence of the  $\mathbf{q}=0$  phonon self-energy  $\Pi(\omega)$ ,<sup>25</sup> whose imaginary part reads as

$$\begin{aligned} \Pi''(\omega) = & \frac{\pi N_s N_b}{N_c} \sum_{\mathbf{k}} |g_{\mathbf{k}, E_{2g}}|^2 \int d\omega' A(\mathbf{k}, \omega' + \omega) \\ & \times A(\mathbf{k}, \omega') [f(\omega' + \omega) - f(\omega')], \end{aligned} \quad (2)$$

where  $N_c$  is the number of sampling points in the Brillouin zone,  $A(\mathbf{k}, \omega) = (1/\pi) \text{Im}[1/[\omega - \epsilon_{\mathbf{k}} - \Sigma(\omega)]]$  is the electron spectral function and  $N_s=2$  and  $N_b=2$  represent, respectively, the spin degeneracy and the  $\sigma$ -band degeneracy. Note that Eq. (2) does not account for the double degeneracy of the two  $E_{2g}$  modes, which, on the other hand, contribute to the superconducting pairing. A similar expression is obtained for the real part of the phonon self-energy, also attainable from the Kramers-Krönig relations. The electron-phonon matrix elements  $g_{\mathbf{k}, E_{2g}}$  can be estimated from the  $E_{2g}$  deformation

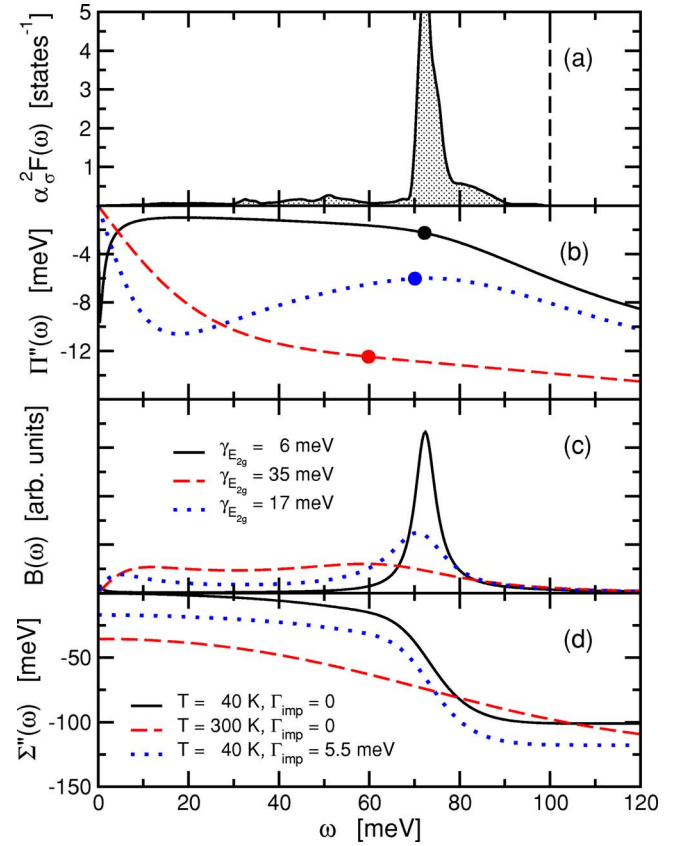


FIG. 1. (Color online) (a) Electron-phonon spectral function  $\alpha_\sigma^2 F(\omega)$  (from Ref. 29). The dashed line represents the unrenormalized phonon frequency  $\Omega_{E_{2g}} = 100$  meV. Panels (b), (c), (d) show, respectively, the imaginary part of the phonon self-energy, the phonon spectral function and the imaginary part of the electronic self-energy for three representative cases.

potential  $D_{E_{2g}} \approx 12$  eV/Å,<sup>1,3,30,31</sup> which is in good approximation  $\mathbf{k}$ -independent close to the Fermi level, and from evaluating the zero point motion lattice displacement  $g_{E_{2g}} = D_{E_{2g}} \sqrt{\langle u^2 \rangle} = 0.39$  eV, taking into account anharmonic effects.<sup>32</sup>

We finally evaluate the phonon spectral function  $B(\omega)$  from the imaginary part of the phonon propagator

$$B(\omega) = -\frac{1}{\pi} \text{Im} \left( \frac{2\Omega_{E_{2g}}}{\Omega_{E_{2g}}^2 - \omega^2 + 2\Omega_{E_{2g}} \Pi(\omega)} \right), \quad (3)$$

where  $\Omega_{E_{2g}}$  is the *unrenormalized* phonon frequency, while the renormalized phonon frequency  $\omega_{E_{2g}}$  and the phonon linewidth  $\gamma_{E_{2g}}$  are simply related to the real and imaginary parts of  $\Pi(\omega)$ ,

$$\omega_{E_{2g}}^2 = \Omega_{E_{2g}}^2 + 2\Omega_{E_{2g}} \Pi'(\omega_{E_{2g}}), \quad (4)$$

$$\gamma_{E_{2g}} = -2(\Omega_{E_{2g}} / \omega_{E_{2g}}) \Pi''(\omega_{E_{2g}}). \quad (5)$$

We assume the unrenormalized  $E_{2g}$  phonon frequency  $\Omega_{E_{2g}} = 100$  meV, close to the top of the phonon spectrum.

In Figs. 1(b) and 1(c), we plot the imaginary part of the phonon self-energy, and the fully renormalized phonon spectrum. The filled symbols mark the values of imaginary parts of the phonon self-energy evaluated at the renormalized phonon frequency  $\omega_{E_{2g}}$  obtained from the self-consistent solution of Eq. (4). At low temperature and in the absence of impurity scattering, the imaginary part of the phonon self-energy shows a monotonic behavior that reflects the corresponding increasing of the electronic damping processes (Fig. 1(d)). Already in this case we predict a relevant value of  $\Pi''(\omega_{E_{2g}})$  and of the phonon linewidth  $\gamma_{E_{2g}} \approx 6$  meV, which is essentially only due to the spectral weight of  $\alpha_{\sigma}^2 F(\omega)$  for  $\omega \leq \omega_{E_{2g}}$ . Things are even more drastic when finite temperature effects or impurity scattering are taken into account. As is well known the imaginary part of the electronic self-energy starts from a finite value at  $\omega=0$  that is reflected in a sudden increase of  $|\Pi''(\omega)|$  and in a significant broadening of the phonon spectrum. Note also the appearance of an incoherent background for  $\omega \leq \omega_{E_{2g}}$  and of a broad shoulder at a very low temperature, in striking agreement with the Raman experimental data. Similar effects were pointed out in Refs. 33 and 34 in the context of the electronic Raman scattering. We would like to stress that the sharp increase of  $|\Pi''(\omega)|$  and the onset of the low temperature shoulder in the phonon spectrum are intrinsic features of the charge response function. As a matter of fact, as noted in Ref. 25, at a first approximation the ratio  $-\Pi''(\omega)/\omega$  is qualitatively similar to the real part of the optical conductivity  $\sigma'(\omega)$ . The low energy sudden enhancement of  $|\Pi''(\omega)|$  and the corresponding shoulder in the phonon spectrum, which arise from the finite value of  $\Sigma''(\omega=0)$ , have thus a strict connection with the appearance of a Drude-like peak in  $\sigma'(\omega)$ . Along this line, the experimental observation of a significant Drude-like scattering rate  $1/\tau \approx 9-37$  meV<sup>35,36</sup> and of the Raman shoulder at low temperatures  $T \sim 40-45$  K<sup>18</sup> points out the actual presence of a small amount of impurity scattering. From the comparison between our results and experimental data, we estimate an impurity scattering rate  $\Gamma_{\text{imp}} \approx 5.5$  meV.

In Fig. 2(a) we show the evolution of the phonon spectral function  $B(\omega)$  at function of the temperature. Increasing temperature leads thus not only to a smearing of the main phonon peak by increasing  $\gamma_{E_{2g}}$  but also to a smearing of the low energy structure, in fair agreement with the experiments. In Figs. 2(b) and 2(c), we show also the temperature dependence of the renormalized phonon frequency  $\omega_{E_{2g}}$  and of the phonon linewidth  $\gamma_{E_{2g}}$ . The agreement with the experimental data is once more remarkable for  $\gamma_{E_{2g}}$ .<sup>19</sup> On the other hand, our analysis underestimates the phonon frequency  $\omega_{E_{2g}} \sim 55-70$  meV (to be compared with the  $\omega_{E_{2g}} \sim 78$  meV from Raman spectroscopy) and predicts a phonon softening as a function of  $T$  that has not been observed. We remind the reader, however, that anharmonic effects are not taken into account here, and that they would lead to a temperature dependent hardening of the  $E_{2g}$  phonon frequency. Since the anharmonic effects were shown to be related to the electron-phonon interaction itself,<sup>30</sup> a correct evaluation of them would require once more the inclusion in a consistent way of the damping electronic processes.

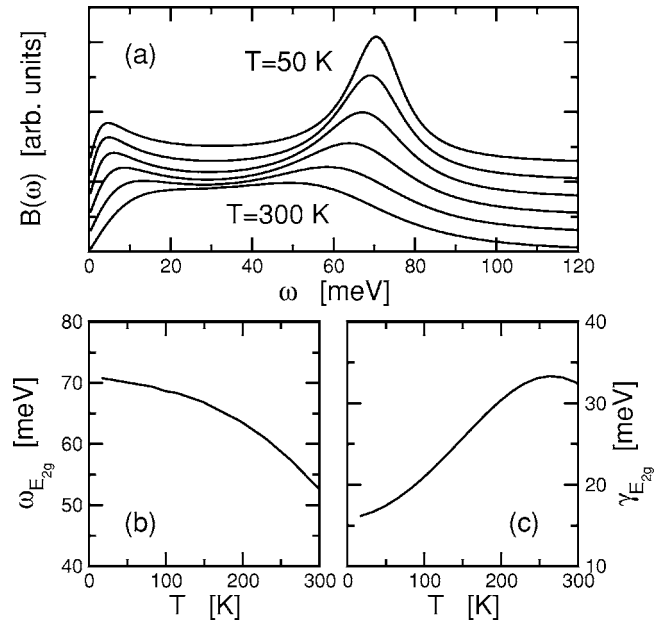


FIG. 2. (a) The phonon spectral function for  $T = 50, 100, 150, 200, 250, 300$  K; (b) temperature dependence of the renormalized phonon frequency  $\omega_{E_{2g}}$ ; (c) temperature dependence of the phonon linewidth  $\gamma_{E_{2g}}$ . Here we considered a small amount of impurity concentration corresponding to  $\Gamma_{\text{imp}} = 5.5$  meV.

As a last point of our analysis we address the evolution of the Raman spectra as a function of the Al doping. Ab initio calculations predict that the electron doping induced by the Al content would fill the two  $\sigma$  bands, leading to a reduction of the electron-phonon coupling. This is expected to result in a steady hardening of the  $E_{2g}$  phonon frequency.<sup>31</sup> Actual Raman measurements are, however, in substantial disagreement with this picture, showing that the phonon hardening occurs via a transfer of the spectral weight from the  $E_{2g}$  peak to another, at the moment unknown, new high energy structure.<sup>16,17</sup> In the following we provide a qualitative scenario where this behavior is naturally explained in terms of finite bandwidth effects that arise when the Fermi level approaches the  $\sigma$  band edge.

A natural modelization to investigate this scenario would be to consider a semi-infinite band system  $\int_{-\infty}^{\infty} d\epsilon \rightarrow \int_{-\infty}^{E_F}$ , where the Fermi energy  $E_F$  plays the role of an energy cutoff for the electronic excitations. However, the correct treatment of the charge conservation and of the asymptotic behavior at  $\omega \rightarrow -\infty$  in the real axis phonon self-energy<sup>25</sup> present different numerical difficulties that make this approach unaffordable. For qualitative insight, we consider thus in the following a simpler model with a symmetric band  $\int_{-E_F}^{E_F}$ , where these numerical problems are overcome. Since the main role is played by the presence of a finite cutoff  $E_F$ , this model is expected to shed a qualitative light also on more realistic cases. In Fig. 3, we show the evolution of the phonon spectral function for  $E_F$  approaching zero for  $T = 40$  K and  $\Gamma_{\text{imp}} = 0$ . For  $E_F$  higher than 60 meV (not shown here) the phonon spectrum presents only a one-peak structure corresponding to the renormalized phonon frequency. As soon as  $2E_F$  decreases, however, this structure rapidly loses spectral weight

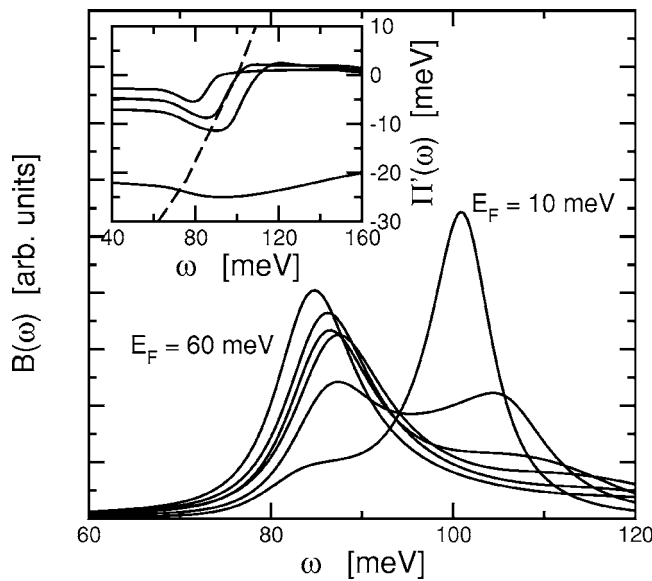


FIG. 3. Evolution of the phonon spectral function by decreasing the  $\sigma$  band Fermi energy for  $T=40$  K and  $\Gamma_{\text{imp}}=0$ . Inset: real part of the phonon self-energy (solid lines) for different  $E_F$ , from top to bottom:  $E_F=10, 20, 30, \infty$  meV. The crossing with the dashed line determines the phonon peaks.

in favor of the unrenormalized phonon frequency  $\Omega_{E_{2g}}$  accompanied by a narrowing of the phonon linewidth. This behavior can be understood by looking at the real part of the phonon self-energy: for  $E_F \rightarrow \infty$  it has a negative minimum at roughly the maximum energy of  $\alpha_\sigma^2 F(\omega)$ , and then it vanishes very slowly for  $\omega \rightarrow \infty$ . Peaks in the phonon spectrum are qualitatively determined by Eq. (4), corresponding to the crossing of  $\Pi'(\omega)$  with the dashed line  $[(\omega^2 - \Omega_{E_{2g}}^2)/2\Omega_{E_{2g}}]$  in the inset of Fig. 3. The finite band edge  $E_F$  is reflected in

a sharp drop of  $\Pi'(\omega)$  due to the cut-off in the particle-hole excitation, with a width roughly given by  $E_F$ . Decreasing  $E_F$  the determination of  $\omega_{E_{2g}}$  according Eq. (4) has an abrupt jump from a renormalized [ $\Pi'(\omega) \neq 0$ ] to the unrenormalized [ $\Pi'(\omega) = 0$ ] value. The crossover between these two regimes occurs roughly at  $E_F \approx 20$  meV, where Eq. (4) has three solutions, corresponding to the two peaks and the middle minimum in the phonon spectrum.

We have been unable to show evidence of this behavior, even at room temperature and in the presence of impurity scattering  $\Gamma_{\text{imp}}=6$  meV, where the large broadening of the phonon spectrum does not permit us to resolve a two-peak structure. One has to take into account, however, that approaching the band edge also the electron DOS and the impurity scattering rate  $\Gamma_{\text{imp}} \propto N(0)$  vanishes. The resemblance of this framework with the experimental results<sup>16,17</sup> is anyway striking, suggesting that finite bandwidth effects are actually the natural explanation of the evolution of the Raman spectrum with Al doping.

In conclusion in this paper we have investigated the phonon Raman spectroscopy data by computing the phonon self-energy of the  $E_{2g}$  mode. We show that the anomalous features of the Raman measurements, namely the huge phonon linewidth, the low energy background, the two-peak structure as function of the Al doping, can be naturally explained by the interplay of the  $E_{2g}$  phonon mode with the whole electron-phonon spectrum which gives rise to damping processes in the electronic excitation and in the  $E_{2g}$  mode itself.

We thank L. Pietronero, G.B. Bachelet, P. Postorino, M. Lavagnini and D. Di Castro, for interesting discussions. We also acknowledge financial support from the MIUR projects FIRB RBAU017S8R and COFIN 2003.

<sup>1</sup>J. M. An and W. E. Pickett, Phys. Rev. Lett. **86**, 4366 (2001).

<sup>2</sup>J. Kortus *et al.*, Phys. Rev. Lett. **86**, 4656 (2001).

<sup>3</sup>T. Yildirim *et al.*, Phys. Rev. Lett. **87**, 037001 (2001).

<sup>4</sup>A. Y. Liu *et al.*, Phys. Rev. Lett. **87**, 087005 (2001).

<sup>5</sup>Y. Kong *et al.*, Phys. Rev. B **64**, 020501(R) (2001).

<sup>6</sup>H. J. Choi *et al.*, Nature **418**, 758 (2002).

<sup>7</sup>F. Bouquet *et al.*, Phys. Rev. Lett. **87**, 047001 (2001).

<sup>8</sup>P. Szabó *et al.*, Phys. Rev. Lett. **87**, 137005 (2001).

<sup>9</sup>F. Giubileo *et al.*, Phys. Rev. Lett. **87**, 177008 (2001).

<sup>10</sup>S. Tsuda *et al.*, Phys. Rev. Lett. **91**, 127001 (2003).

<sup>11</sup>R. S. Gonnelli *et al.*, Phys. Rev. Lett. **89**, 247004 (2003).

<sup>12</sup>J. S. Slusky *et al.*, Nature **410**, 343 (2001).

<sup>13</sup>K.-P. Bohnen *et al.*, Phys. Rev. Lett. **86**, 5771 (2001).

<sup>14</sup>J. Hlinka *et al.*, Phys. Rev. B **64**, 140503(R) (2001).

<sup>15</sup>A. F. Goncharov *et al.*, Phys. Rev. B **64**, 100509(R) (2001).

<sup>16</sup>P. Postorino *et al.*, Phys. Rev. B **65**, 020507(R) (2001).

<sup>17</sup>B. Renker *et al.*, Phys. Rev. Lett. **88**, 067001 (2002).

<sup>18</sup>J. W. Quilty *et al.*, Phys. Rev. Lett. **88**, 087001 (2002).

<sup>19</sup>H. Martinho *et al.*, Solid State Commun. **125**, 499 (2003).

<sup>20</sup>A. Shukla *et al.*, Phys. Rev. Lett. **90**, 095506 (2003).

<sup>21</sup>M. Lazzeri *et al.*, Phys. Rev. B **68**, 220509(R) (2003).

<sup>22</sup>M. Calandra and F. Mauri, Phys. Rev. B **71**, 064501 (2005).

<sup>23</sup>P. B. Allen, Phys. Rev. B **6**, 2577 (1972).

<sup>24</sup>R. Zeyher and G. Zwirnagl, Solid State Commun. **66**, 617 (1988).

<sup>25</sup>F. Marsiglio *et al.*, Phys. Rev. B **45**, 9865 (1992).

<sup>26</sup>C. O. Rodriguez *et al.*, Phys. Rev. B **42**, 2692 (1990).

<sup>27</sup>B. Friedl *et al.*, Phys. Rev. Lett. **65**, 915 (1990).

<sup>28</sup>F. Marsiglio *et al.*, Phys. Rev. B **37**, 4965 (1988).

<sup>29</sup>A. A. Golubov *et al.*, J. Phys.: Condens. Matter **14**, 1353 (2002).

<sup>30</sup>L. Boeri *et al.*, Phys. Rev. B **65**, 214501 (2002).

<sup>31</sup>G. Profeta *et al.*, Phys. Rev. B **68**, 144508 (2003).

<sup>32</sup>L. Boeri *et al.*, Phys. Rev. B **71**, 012501 (2005).

<sup>33</sup>A. Zawadowski and M. Cardona, Phys. Rev. B **42**, 10732 (1990).

<sup>34</sup>T. Dahm *et al.*, Phys. Rev. B **59**, 14740 (1999).

<sup>35</sup>J. J. Tu *et al.*, Phys. Rev. Lett. **87**, 277001 (2001).

<sup>36</sup>R. A. Kaindl *et al.*, Phys. Rev. Lett. **88**, 027003 (2002).